Contributions of *BMPR2* Mutations and Extrinsic Factors to Cellular Phenotypes of Pulmonary Arterial Hypertension Revealed by Induced Pluripotent Stem Cell Modeling

To the Editor:

Reduced BMPR2 (bone morphogenetic protein receptor 2) signaling is central to the pathobiology of pulmonary arterial hypertension (PAH). However, the reduced penetrance of *BMPR2* mutations in families suggests that other factors are required to establish disease (1). To date, it has proved difficult to elucidate these factors because of a lack of appropriate models. Sa and colleagues (2) developed an induced pluripotent stem cell (iPSC)-derived endothelial cell (iPSC-EC) model of PAH that recapitulated some of the previously described phenotypes of patient-derived pulmonary artery endothelial cells (PAECs), as well as appropriate responsiveness to Elafin and FK506 (2). This demonstrated a potential utility of iPSCs in modeling PAECs in PAH. However, other phenotypes such as inner mitochondrial membrane (IMM) hyperpolarization could not be recapitulated. Therefore, there is a need to better understand the contribution of *BMPR2* mutations to PAH-associated phenotypes and the requirement for other factors in this process. Two advantages of iPSCs in disease modeling are their amenability to genome editing and their differentiation into specific cell types under serum-free, chemically defined conditions. This allows the assessment of the effect of a *BMPR2* mutation without the confounding effects of genetic differences between cell lines, and the determination of the effect of controlled exposure to extrinsic factors that may influence the acquisition of a diseased state. In addition, no iPSC–smooth muscle cell (SMC) model of PAH has yet been described. We have addressed these issues.

Methods

Using clustered regularly interspaced short palindromic repeats–Cas9–mediated homologous recombination in a wild-type iPSC line, two isogenic sublines carrying either a known causal *BMPR2* mutation (W9X; referred to as C2 W9X$^{+/-}$) or a deletion of exon 1 (C2 ΔExon1) were generated. Serum-free, chemically defined iPSC differentiation protocols were used to generate iPSC-derived SMCs (iPSC-SMCs) and iPSC-ECs. This was achieved by differentiating iPSCs into iPSC-SMCs via a lateral plate mesoderm, paraxial mesoderm, or neural ectoderm lineage followed by 12 days in TGF-β1 (transforming growth factor β 1) and PDGF-BB (platelet-derived growth factor BB) ± BMP4 (bone morphogenetic protein 4) (Figure 1A) (3), and into ECs via FGF-2 (fibroblast growth factor 2)–induced, BMP4-induced, and LY294002-induced mesoderm followed by FGF-2 and VEGF (vascular endothelial growth factor) ± BMP4. iPSC-SMCs were compared with adult distal and proximal pulmonary artery smooth muscle cells (PASMCs) by microarray analysis. Cells were used postdifferentiation and in chemically defined conditions, and exposed to additional factors such as serum, BMP4, and TNFα (tumor necrosis factor α). Key PAH-associated cellular phenotypes, including altered apoptosis (via caspase cleavage and annexin/propidium iodide staining), proliferation (via DNA content and cell counts), and IMM polarization (via tetramethylrhodamine ethyl ester staining), which are cellular changes common to both SMCs and ECs (4), were assessed.

Results and Discussion

The *BMPR2* mutations introduced into C2-iPSCs resulted in *BMPR2* haploinsufficiency in an otherwise isogenic background compared with the wild-type parent iPSC line. This approach removed the effects that different genetic modifiers (5) may have on the penetrance of cellular phenotypes.

Derivation of iPSC-SMCs and iPSC-ECs that perfectly represent adult PASMCs and PAECs is yet to be achieved. Therefore, our goal was to generate iPSC-SMCs that recapitulated some of the important functional responses of adult-derived distal PASMCs, as well as iPSC-ECs with enhanced expression of arterial markers, that could be used as surrogates for adult pulmonary vascular cells. The lineage-specific differentiation protocols used generated iPSC-SMCs expressing SMA (smooth muscle actin), CALPONIN, and MYH11 (myosin heavy chain 11) (Figure 1A and data not shown) that had a contractile phenotype (data not shown), as well as iPSC-ECs, which were enriched for arterial-specific EC markers including *ACVRL1* (activin A receptor like type 1), *CLDN5* (claudin 5), *EFNB2* (ephrin B2), *NOTCH1*, *JAG* (Jagged)-1, and *JAG2* and able to form vascular networks (data not shown) (6). Principle component analysis of microarray gene expression data for 171 SMC-associated genes showed that lateral plate mesoderm-SMCs were more similar to distal PASMCs compared with paraxial mesoderm-derived and neural ectoderm-derived SMCs (Figure 1B). In addition, lateral plate mesoderm-SMCs were not growth suppressed by BMP4 (50 ng/ml) and were less apoptotic when treated with BMP4, similar to the responses previously described in distal PASMCs from donors (Figures 1C and 1D) (7).

Under these serum-free, chemically defined conditions, *BMPR2* heterozygosity alone was sufficient to cause reduced apoptosis and increased proliferation in iPSC-SMCs (Figures 2A and 2B). However, *BMPR2* heterozygosity in iPSC-ECs required additional exposure to serum to manifest increased proliferation

Supported by funding from the British Heart Foundation (BHF; project grant PG/14/31/30786 and program grant RG/13/4/30107), the Cambridge National Institute for Health Research Biomedical Research Centre, the Dinosaur Trust, Fondation Leducq, the Medical Research Council (MRC Experimental Challenge Award MR/KO20919/1), Pulmonary Hypertension Association UK, and Fight for Sight and the Robert McAlpine Foundation. N.W.M. was supported by a BHF Chair Award (CH/09/001/25945) and F.N.K. was supported by a BHF PhD studentship (FS/13/51/30636) and a travel grant from St. Catharine's College Cambridge. N.W.M. and A.A.R. would also like to acknowledge support from the BHF Centre of Regenerative Medicine, Oxford and Cambridge (RM/13/3/30159); the BHF Centre for Research Excellence (RE/13/6/30180); the BHF IPAH cohort grant (SP/12/12/29836); Selwyn and St. Catharine's Colleges, Cambridge; and a Pfizer European Young Researcher of the Year award (A.A.R.).

Author Contributions: F.N.K. and C-H.C. designed and performed experiments, analyzed data, and wrote the manuscript; C.J.Z.H. designed and performed experiments and analyzed data; B.K., C.C., and B.J.D. performed experiments; F.S. and S.S. analyzed data; N.W.M. designed experiments and wrote the manuscript; A.A.R. designed and performed experiments, analyzed data, and wrote the manuscript; F.N.K., C-H.C., and C.J.Z.H. contributed equally to the work; N.W.M. and A.A.R. supervised the work; and all authors read the manuscript and approved the final version.

Originally Published in Press as DOI: 10.1164/rccm.201801-0049LE on March 16, 2018

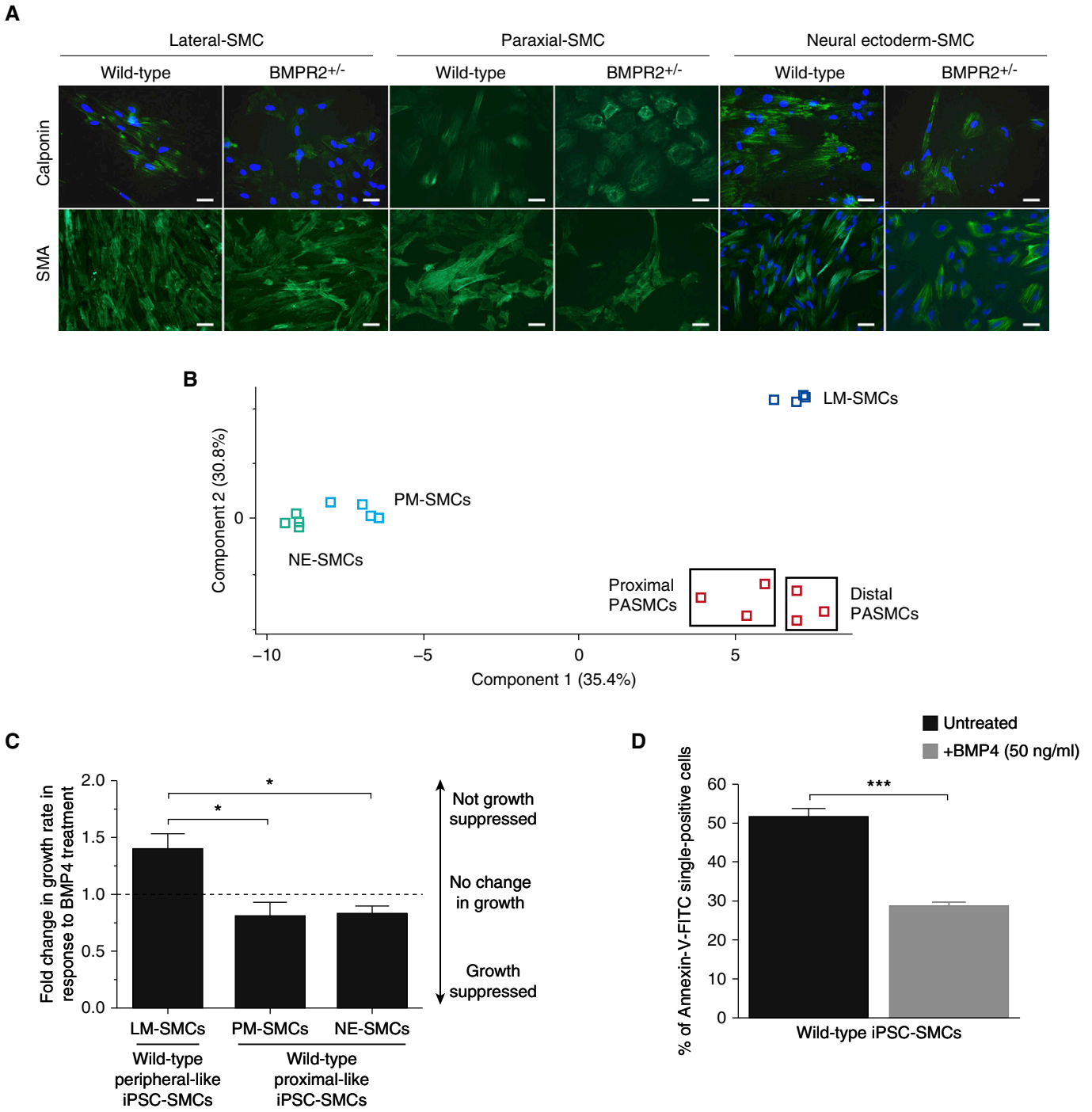

Figure 1. Generation of pulmonary artery smooth muscle cell (PASMC)-like induced pluripotent stem cell (iPSC)-derived smooth muscle cells (SMCs). (*A*) Wild-type and *BMPR2*$^{+/-}$ iPSCs differentiated into iPSC-SMCs from lateral plate mesoderm (LM), paraxial mesoderm (PM), and neuroectoderm (NE) express SMA (smooth muscle actin) and calponin (green), (DAPI; blue) (scale bars, 20 μm). (*B*) Gene expression patterns of all samples (human PASMCs, PM-SMCs, NE-SMCs, and LM-SMCs) were analyzed using Illumina HumanHT-12 v4 Expression BeadChip microarrays. Gene expression patterns of samples were sorted based on similarity by hierarchical clustering. For this analysis, 171 SMC-specific genes were selected based on the wikipathway database (WikiPathway WP2064 revision 47071). The two-dimensional principal component analysis for differential gene expression is plotted in *B*. The red squares inside black boxes represent PASMCs, dark blue squares represent LM-SMCs, green squares represent NE-SMCs, and light blue squares represent PM-SMCs. (*C*) LM-SMCs are not growth suppressed by BMP4 (50 ng/ml), unlike PM- and NE-SMCs. (*D*) The apoptotic response in wild-type LM-SMCs is reduced in the presence of exogenous BMP4 (50 ng/ml), as previously described for distal PASMCs. Data in *C* and *D* are presented as mean ± SEM of three biological replicates (*$P < 0.05$; ***$P < 0.001$; one-way ANOVA [*C*] and Student's *t* test [*D*]). BMP = bone morphogenetic protein; BMPR = BMP receptor; FITC = fluorescein isothiocyanate.

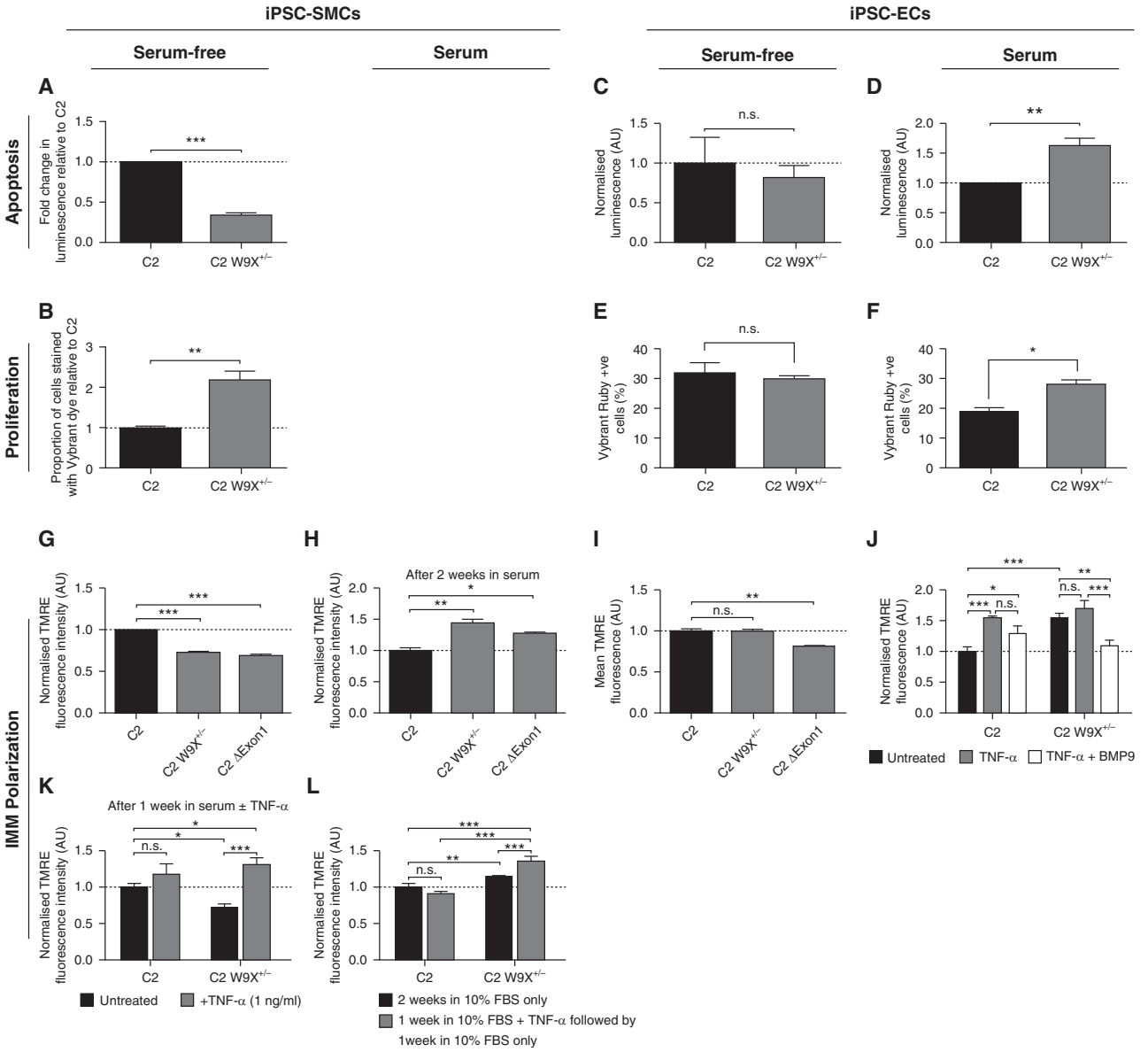

Figure 2. Effect of *BMPR2* (bone morphogenetic protein receptor 2) heterozygosity on proliferation, apoptosis, and inner mitochondrial membrane (IMM) polarization of induced pluripotent stem cell (iPSC)-derived smooth muscle cells (SMCs) and iPSC–endothelial cells (ECs). (*A* and *B*) C2 W9X$^{+/-}$ iPSC-SMCs are (*A*) significantly less apoptotic and (*B*) more proliferative than wild-type C2 iPSC-SMCs under serum-free conditions, assessed using the Caspase-3/7 Glo assay (*A*) and by measuring double-stranded DNA content by Vybrant DyeCycle Ruby staining (*B*). (*C* and *E*) In contrast, there was no significant difference in (*C*) apoptosis and (*E*) proliferation between C2 and C2 W9X$^{+/-}$ iPSC-ECs under serum-free conditions. (*D* and *F*) C2 W9X$^{+/-}$ iPSC-ECs became significantly more (*D*) apoptotic and (*F*) proliferative relative to isogenic wild-type C2 iPSC-ECs after exposure to 10% FBS for 1 week. (*G*) Serum-free *BMPR2*$^{+/-}$ iPSC-SMCs display a hypopolarized IMM compared with isogenic wild-type cells, assessed using tetramethylrhodamine ethyl ester (TMRE) staining and flow cytometry. (*H* and *K*) *BMPR2*$^{+/-}$ iPSC-SMCs became hyperpolarized compared with isogenic wild-type cells (*H*) after 2 weeks of exposure to serum or (*K*) after 1 week of exposure to serum and TNFα (tumor necrosis factor α) (1 ng/ml). (*L*) After 1 week of exposure to serum + TNFα, TNFα was removed and all cells were cultured for 1 further week in serum only to see whether the polarization state would recover. The polarization state of *BMPR2*$^{+/-}$ iPSC-SMCs did not normalize and was significantly higher than exposure to serum only for 2 weeks, and was also significantly higher than in isogenic wild types treated the same way. (*I* and *J*) *BMPR2*$^{+/-}$ iPSC-ECs (*I*) do not have a hyperpolarized IMM relative to the isogenic wild-type under serum-free conditions but (*J*) become significantly hyperpolarized after exposure to serum for 1 week. Wild-type iPSC-ECs showed significantly higher TMRE fluorescence after TNFα treatment (1 ng/ml), suggesting that TNFα increases IMM hyperpolarization. Cotreatment of C2 W9X$^{+/-}$ iPSC-ECs with TNFα (1 ng/ml) and BMP9 (1 ng/ml) for 1 week resulted in significantly reduced TMRE fluorescence, and hence IMM polarization, compared with the effect of TNFα alone. Data are presented as mean ± SEM of the results from three independent differentiations (*A–F*) and three technical replicates per differentiation (*$P < 0.05$; **$P < 0.01$; ***$P < 0.001$; Student's *t* test [*A–F*], one-way ANOVA [*G–I*], or two-way ANOVA [*J–L*]). AU = arbitrary units; BMP9 = bone morphogenetic protein 9; C2 = control 2, patient cell line; C2 δExon 1 = C2 carrying deletion of exon 1 in the gene *BMPR2*; C2 W9X = C2 carrying a W9X mutation in the gene *BMPR2*; FBS = fetal bovine serum; n.s. = not significant.

and apoptosis (Figures 2C–2F). These findings were confirmed by performing cell counts to assess proliferation, and annexin-V–fluorescein isothiocyanate propidium iodide staining to measure apoptosis (data not shown). Taken together, these results demonstrate a clear difference in the contribution of *BMPR2* heterozygosity to establishing disease phenotypes in SMCs and ECs, and therefore highlight an important difference between these cell types. In contrast, neither cell type displayed hyperpolarized IMMs as they emerged from the serum-free iPSC differentiation protocols (Figures 2G and 2I). Only after serum ± TNFα exposure for 1 week for iPSC-ECs (Figure 2J), and serum + TNFα exposure for 1 week or serum-only for 2 weeks for iPSC-SMCs (Figures 2H, 2K, and 2L), did these cells acquire IMM hyperpolarization. IMM hyperpolarization is a key factor in pulmonary vascular remodeling, but how a hyperpolarized state is established in the context of *BMPR2* heterozygosity was not known. Recently, BMP9 was shown to reverse PAH in rodent models, mainly via its action on PAECs (8). In iPSC-ECs, IMM hyperpolarization could be prevented by exposure to BMP9 (1 ng/ml; Figure 2J), potentially exposing one of the possible modes of action of BMP9 in reversing PAH. Remarkably, $BMPR2^{+/-}$ iPSC-SMCs demonstrated prolonged hyperpolarization despite withdrawal of TNFα (Figure 2L). This suggests that transient exposure to a disease-triggering agent may be sufficient to drive the progression of disease in a *BMPR2* mutation carrier.

The significance of these findings is that this iPSC system can be used to address the controversial question of whether genetic reduction of BMPR2 alone is necessary and/or sufficient for establishing the major cellular phenotypes associated with PAH. This would be extremely difficult to address in patient-derived primary cells. The use of specialized differentiation protocols with minimal interference from extrinsic factors allowed the effect of *BMPR2* heterozygosity in SMCs and ECs to be shown definitively. Extrinsic factors were then added in a highly controlled manner to show their effect on establishing PAH-associated cellular phenotypes. In essence, it was possible to transition cells from a prediseased to a diseased state, opening the way to discovering new druggable pathways to prevent or reverse PAH. Although the generation of pulmonary SMCs and ECs from iPSCs is yet to be achieved, the differentiation protocols used in this study produced cells that recapitulated key phenotypes found in diseased adult PASMCs and PAECs. Thus, these protocols will have a broad effect for those modeling pulmonary vascular diseases, and also for those using pulmonary organoids and pulmonary artery–on-chip technologies to study epithelial–endothelial cell interactions in the alveoli and for drug screening. Finally, this study defines an iPSC-derived SMC model of PAH. Only EC and mesenchymal iPSC models of PAH have been described previously, and the mesenchymal model did not recapitulate the pro-proliferative phenotype of SMCs from patients with PAH (9). ■

Author disclosures are available with the text of this letter at www.atsjournals.org.

Fedir N. Kiskin, M.Res.*
C-Hong Chang, Ph.D.*
Christopher J. Z. Huang, M.Phil.*
University of Cambridge
Cambridge, United Kingdom

Baraa Kwieder, M.Sc.
University of Cambridge
Cambridge, United Kingdom
and
British Heart Foundation Cambridge Centre of Research Excellence
Cambridge, United Kingdom

Christine Cheung, Ph.D.
Nanyang Technological University
Singapore
and
Cambridge Stem Cell Institute
Cambridge, United Kingdom

Benjamin J. Dunmore, Ph.D.
Felipe Serrano, Ph.D.
University of Cambridge
Cambridge, United Kingdom

Sanjay Sinha, Ph.D.
University of Cambridge
Cambridge, United Kingdom
British Heart Foundation Cambridge Centre of Research Excellence
Cambridge, United Kingdom
Cambridge Stem Cell Institute
Cambridge, United Kingdom
and
British Heart Foundation Oxford and Cambridge Centre of Regenerative Medicine
Oxford, United Kingdom and Cambridge, United Kingdom

Nicholas W. Morrell, M.D.‡
Amer A. Rana, Ph.D.‡
University of Cambridge
Cambridge, United Kingdom
British Heart Foundation Cambridge Centre of Research Excellence
Cambridge, United Kingdom
and
British Heart Foundation Oxford and Cambridge Centre of Regenerative Medicine
Oxford, United Kingdom and Cambridge, United Kingdom

*These authors contributed equally to this work.

‡Joint senior authors.

ORCID IDs: 0000-0002-6984-9622 (F.N.K.); 0000-0002-2330-4643 (A.A.R.).

References

1. Soon E, Crosby A, Southwood M, Yang P, Tajsic T, Toshner M, *et al*. Bone morphogenetic protein receptor type II deficiency and increased inflammatory cytokine production: a gateway to pulmonary arterial hypertension. *Am J Respir Crit Care Med* 2015;192:859–872.
2. Sa S, Gu M, Chappell J, Shao NY, Ameen M, Elliott KA, *et al*. Induced pluripotent stem cell model of pulmonary arterial hypertension reveals novel gene expression and patient specificity. *Am J Respir Crit Care Med* 2017;195:930–941.
3. Cheung C, Bernardo AS, Trotter MW, Pedersen RA, Sinha S. Generation of human vascular smooth muscle subtypes provides insight into embryological origin-dependent disease susceptibility. *Nat Biotechnol* 2012;30:165–173.
4. Pullamsetti SS, Savai R, Seeger W, Goncharova EA. Translational advances in the field of pulmonary hypertension: from cancer biology to new pulmonary arterial hypertension therapeutics: targeting cell growth and proliferation signaling hubs. *Am J Respir Crit Care Med* 2017;195:425–437.
5. Gu M, Shao NY, Sa S, Li D, Termglinchan V, Ameen M, *et al*. Patient-specific iPSC-derived endothelial cells uncover pathways that protect

against pulmonary hypertension in BMPR2 mutation carriers. *Cell Stem Cell* 2017;20:490–504.
6. Marcelo KL, Goldie LC, Hirschi KK. Regulation of endothelial cell differentiation and specification. *Circ Res* 2013;112:1272–1287.
7. Yang X, Long L, Southwood M, Rudarakanchana N, Upton PD, Jeffery TK, *et al*. Dysfunctional Smad signaling contributes to abnormal smooth muscle cell proliferation in familial pulmonary arterial hypertension. *Circ Res* 2005;96:1053–1063.
8. Long L, Ormiston ML, Yang X, Southwood M, Gräf S, Machado RD, *et al*. Selective enhancement of endothelial BMPR-II with BMP9 reverses pulmonary arterial hypertension. *Nat Med* 2015;21:777–785.
9. West JD, Austin ED, Gaskill C, Marriott S, Baskir R, Bilousova G, *et al*. Identification of a common Wnt-associated genetic signature across multiple cell types in pulmonary arterial hypertension. *Am J Physiol Cell Physiol* 2014;307:C415–C430.

The Effects of Timed Light Exposure in Critically Ill Patients: A Randomized Controlled Pilot Clinical Trial

To the Editor:

The circadian timing system aligns genetic, physiologic, and behavioral rhythms to solar time (1). The master pacemaker of the body is normally synchronized, or entrained, to solar time each day by environmental *zeitgebers* ("time givers"), particularly the light–dark cycle (2). When sleep is mistimed in relation to the endogenous circadian rhythm, the circadian regulation of the human transcriptome is disrupted (3) and health is adversely affected (4, 5).

Critically ill patients exhibit profound disruptions of circadian rhythmicity, most commonly in the form of a phase delay (6–8). The ICU environment has been implicated in the pathogenesis of these dysrhythmias, but evidence for this hypothesis has been lacking. Indirect support for this hypothesis derives from data showing that the light–dark cycle of a typical ICU is consistently weak and phase-delayed relative to the solar cycle (9). To more directly test this hypothesis, we conducted a randomized controlled pilot study in critically ill patients (ClinicalTrials.gov identifier: NCT01284140) to determine the effect of timed light exposure (TLE) on the timing and amplitude of the 24-h 6-sulfatoxymelatonin (aMT6s) rhythm. Some of the results of this study have been previously reported in the form of an abstract (10).

Methods

We enrolled adult (≥18 yr old) patients being treated in the medical ICUs at the University of Iowa and the University of Chicago for shock and/or respiratory failure requiring mechanical ventilation. Exclusion criteria included recent major surgery or general anesthesia, neuromuscular blockers, oliguria (<500 ml/d), major sensory impairments, acute neurologic disease, shift work, narcolepsy, drug overdose, and known bipolar disorder, schizophrenia, or schizoaffective disorder. The universities' institutional review boards approved the study, and written informed consent was obtained from participants or their authorized representatives.

Patients were randomly assigned to 48 hours of usual care or TLE. The intervention began the next morning, on Day 1, and enforced a specific period of enhanced light exposure from 9:00 A.M. to noon. The initial target of 5,000 lux ($n = 10$) administered by light box (Sunsation; SunBox Co.) was reduced to 400–700 lux ($n = 14$) to simplify administration, given evidence that the effects of light intensity on phase resetting are nonlinear and enhanced by prior dim light exposure (2, 11). All subjects receiving mechanical ventilation were ventilated in the assist-control mode at night and received targeted sedation according to institutional protocol (12).

We used the 24-hour profile of urinary aMT6s to assess circadian phase and amplitude (6, 13). Urine samples were collected hourly for 24 hours beginning at 8 A.M. on Day 1. This sampling procedure was repeated on the morning of Day 3, yielding two separate 24-hour profiles for each subject. For each 24-hour profile, total daytime (07:00–23:00) and nighttime (23:00–07:00) aMT6s excretion was determined by calculating the area under the curve for the interval.

The primary outcome measures were the change in timing of the acrophase (fitted maximum) of normalized aMT6s excretion between Day 1 and Day 3 in each group. Nonlinear regression using the least-squares approach (Prism 7; GraphPad Software, Inc.) was used to fit a single 24-hour cosine curve to all normalized data in each group on each day. Model parameters of acrophase and amplitude and their SEs were derived from these curves.

Between-group differences in baseline characteristics and ambient light exposure were tested using a *t* test or Mann-Whitney *U* rank sum test, as appropriate. Linear regression was used to examine the relationship between total aMT6s excretion and subject characteristics. Differences in proportions between the two groups were tested using Fisher's exact test. An unpaired *t* test was used to compare best-fit values of rhythm amplitude between groups. ANOVA with repeated measures was used to examine the effect of treatment group and time on individual rhythm amplitude. Data were analyzed according to the intention-to-treat principle. All statistical tests were two-sided, and a *P* value of less than 0.05 was considered significant.

Results

Table 1 shows the clinical characteristics of the subjects. At baseline, the circadian rhythm of the cohort ($n = 21$) was phase

B.K.G. received support for this study from K23HL088020 from the NHLBI, NIH. The Institute for Clinical and Translational Science at the University of Iowa is supported by the NIH Clinical and Translational Science Award program, grant U54TR001356. The Clinical and Translational Science Award program is led by the NIH's National Center for Advancing Translational Sciences. This publication's contents are solely the responsibility of the authors and do not necessarily represent the official views of the NIH.

Author Contributions: B.K.G. takes responsibility for the content of the manuscript and was involved in the conception, hypothesis delineation, and design of the study; the acquisition and analysis of the data; and writing the paper. S.B.P. was involved in the design of the study and the acquisition of the data and reviewed the paper for critical content. E.V.C. was involved in the design of the study, the analysis of the data, and writing the paper. A.S.P. was involved in the design of the study and the acquisition of the data and reviewed the paper for critical content. J.B.H. was involved in the design of the study and the analysis of the data, and reviewed the paper for critical content. J.Z. was involved in the analysis of the data and writing the article.

Originally Published in Press as DOI: 10.1164/rccm.201801-0170LE on March 12, 2018